Available online at www.sciencedirect.com
ScienceDirect
Journal of Nuclear Materials 367–370 (2007) 960–965
journal of nuclear materials
www.elsevier.com/locate/jnucmat

Deformation-induced martensite formation and dislocation channeling in neutron-irradiated 316 stainless steel

N. Hashimoto *, T.S. Byun

Oak Ridge National Laboratory, 1 Bethel Valley Road, Metals and Ceramics Division, P.O. Box 2008, BLDG 4500S, Oak Ridge, TN 37831-6136, USA

Abstract

The deformed microstructure in 316 stainless steel (316SS) after neutron irradiation in the range of 65–100 °C to 0.78 dpa was investigated by transmission electron microscopy (TEM). Deformation-induced martensite transformation and dislocation channeling were observed at irradiation dose higher than 0.1 dpa. Estimation of the resolved shear stress (RSS) associated with each dislocation channel indicated a tendency for the RSS and channel width to be greatest when the angle between tensile axis and slip plane normal is around 45°. Furthermore, channel width increased with increasing RSS, indicating that the most extensive localized channel deformation tends to occur at a high RSS level. Deformation-induced martensite phase was found at various strain levels even at room temperature and tends to be exhibited mainly at intersections of channels. This suggests that a very high stress could lead to the $\gamma \rightarrow \alpha$ martensite formation by the spreading of a Shockley partial dislocation over successive $\langle 1\,1\,1\rangle_{fcc}$ planes.

1. Introduction

Low temperature neutron irradiation often results in a decrease in tensile ductility, leading to the loss of strain hardening capacity, especially at higher doses (>0.1 dpa) [1–4]. These mechanical property changes are usually attributed to the presence of irradiation-induced defect clusters such as black dots, faulted dislocation loops (Frank loop), and stacking fault tetrahedra (SFT), that act as obstacles to dislocation motion during deformation. A general tendency has been observed in many irradiated materials for the radiation-induced defect structure to promote inhomogeneous deformation: dislocation channeling, twinning, and martensite formation, especially in low stacking fault energy (SFE) materials such as austenitic stainless steels [5].

During deformation the mobile dislocations cut, annihilate, and/or combine with the defect clusters on the slip plane during glide. Subsequent dislocations will tend to glide more easily along this same path, cleaning out additional defect clusters resulting in a channel free of defects. The increased slip band spacing that results from dislocation channeling reduces macroscopic displacement over a fixed dimension and hence reduces bulk ductility. Dislocation channel deformation has been seen in many low-SFE materials, but the understanding of radiation-induced hardening behavior is insufficient.

* Corresponding author. Tel.: +1 865 576 2714; fax: +1 865 574 0641.
E-mail address: hashimoton@ornl.gov (N. Hashimoto).

0022-3115/$ - see front matter © 2007 Published by Elsevier B.V.
doi:10.1016/j.jnucmat.2007.03.204

Therefore, it is important to clarify the relationship between irradiation-induced hardening and inhomogeneous deformation mode in neutron-irradiated low-SFE materials.

2. Experimental procedure

Commercial-purity 316SS was used in this study. The chemical composition of 316SS is Fe–17.15Cr–13.45Ni–2.34Mo–0.1Cu–1.86Mn–0.059C–0.57Si–0.018S–0.024P–0.02Co–0.031N (wt%). Specimens were annealed at 1050 °C for 30 min. Custom-designed sheet tensile specimens with a gauge section of 8.0 mm long, 1.5 mm wide, and 0.25 mm thick and an overall length of 17.0 mm were irradiated in the range of 65–100 °C in the Hydraulic Tube facility of the High Flux Isotope Reactor (HFIR). The irradiation exposures ranged from 1.1×10^{21} to 6.3×10^{24} n m^{-2}, $E > 0.1$ MeV, corresponding to nominal atomic displacement levels of 0.0001–0.78 dpa. All tensile tests were conducted at room temperature at a crosshead speed of 0.008 mm s^{-1}, corresponding to an initial specimen strain rate of 10^{-3} s^{-1}. The 0.2% offset yield strength (YS), ultimate tensile strength (UTS), uniform elongation (UE), and total elongation (TE) were calculated from the engineering load-elongation curves. Rectangular pieces were cut from the uniform gauge sections of the tensile-tested (broken) specimens for examination by TEM. Electron microscopy observation was performed at Oak Ridge National Laboratory (ORNL) with a JEM-2000FX and a Philips-CM30 transmission electron microscope operating at 200 kV and 300 kV, respectively.

3. Results and discussion

3.1. Engineering tensile and strain-hardening behavior in neutron-irradiated 316SS

Fig. 1 shows engineering stress–strain curves for 316SS irradiated up to 0.78 dpa. The YS and the UTS increased with increasing irradiation dose. There was no yield point drop in the unirradiated specimen and in specimens irradiated to the lower doses (<0.01 dpa). A yield drop appeared at 0.01 dpa and increased in size with increasing dose. In addition, the decrease of hardening capability is evident, especially at higher irradiation doses (0.01–0.79 dpa). Fig. 2 shows the strain-hardening rate versus true stress curves (Kocks–Mecking plots) for 316SS before and after irradiation. Very high

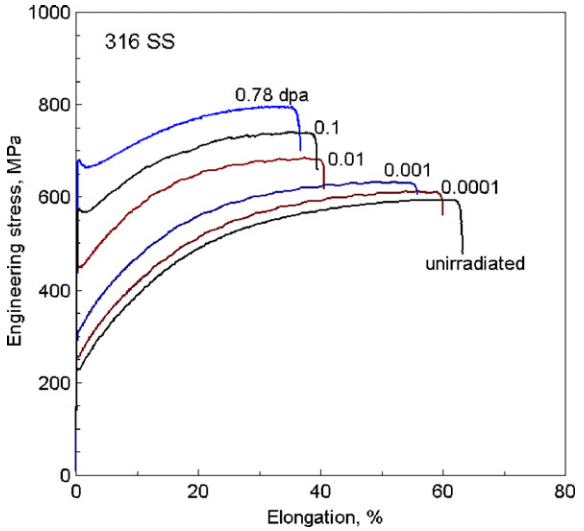

Fig. 1. Room temperature engineering stress–strain curves for 316SS irradiated up to 0.78 dpa.

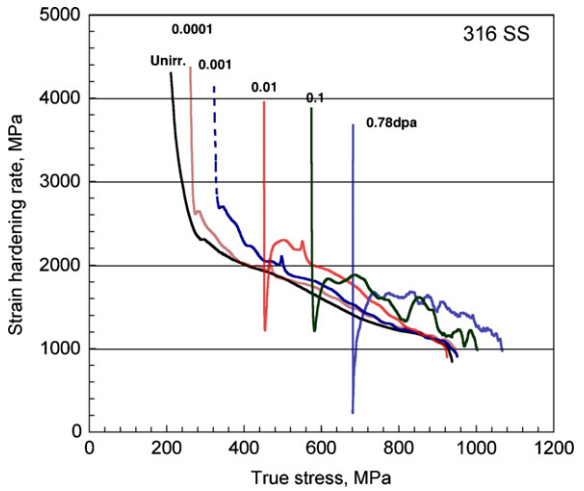

Fig. 2. Room temperature strain-hardening rate versus true stress curves for 316SS before and after irradiation.

strain-hardening rates were found at the onset of deformation, and the strain-hardening rate decreased rapidly with increasing stress. In the 316SS unirradiated and irradiated to lower doses (<0.001 dpa), the strain-hardening rate decreased with stress to the end of deformation. On the other hand, the strain-hardening curve of the 316SS irradiated to higher doses (>0.01 dpa) displayed a yield drop behavior. The first parabolic hardening trend ended after a little increase of stress, where the strain-hardening rate became a minimum value. From this point, the strain-hardening rate increased approximately 800–1600 MPa with a small increase of stress (50–

100 MPa), and then, gradually decreased with increasing stress to the end of deformation. This prompt decrease and small increase of strain-hardening rate at higher irradiation doses could be due to localized deformation behavior.

3.2. Microstructural evolution of neutron-irradiated 316SS

Neutron irradiation at low temperature produced a high number density ($\sim 10^{23}$ m^{-3}) of very small defect clusters ($\sim$3 nm) in the specimen. In neutron-irradiated 316SS there were no SFT observed but a high number density of black dots and Frank loops at the highest dose (0.78 dpa). Measured defect cluster parameters are listed in Table 1. From simple geometric considerations of a dislocation traversing a slip plane which intersects randomly distributed obstacles of diameter d and atomic density N, the increase in the uniaxial tensile stress for polycrystalline specimens ($\Delta\sigma$) in a material is given by the well-known dispersed barrier hardening equation [1], $\Delta\sigma = M\alpha\mu b(\mathrm{Nd})^{1/2}$, where μ is the shear modulus, b is the magnitude of the Burgers vector of the glide dislocation ($a_0/\sqrt{2}$ for FCC, where a_0 is the lattice parameter), M is the Taylor factor (3.06), and α is average barrier strength of the radiation-induced defect clusters. In this study, neutron-irradiated 316SS exhibited a mixture of defect clusters, so that the barrier strength for different types of cluster could not be estimated. Instead, the average barrier strength for clusters was estimated to be 0.5. This barrier strength is probably due to the existence of Frank loops. The estimated α value of a Frank loop has been reported to be 0.5 for neutron-irradiated 316LN irradiated at low temperatures [6].

3.3. Microstructure of neutron-irradiated 316SS after deformation

Fig. 3 shows the general deformation microstructure at low magnification after irradiation up to 0.79 dpa. Dislocation channeling is visible as narrow bands, which have been largely cleaned of the fine defect structure. Dislocation channeling can be practically distinguished from twinning: streaks arising from twin boundaries should be found in the diffraction pattern because the twin is a very thin platelet. The deformed microstructure of 316SS irradiated to lower than 0.01 dpa consisted of a mixture of dislocation bands, tangles, and twins. However, microstructure of the deformed 316SS irradiated to higher than 0.1 dpa mainly showed twinning and dislocation channeling, which is coincident with prompt plastic instability at yield. Dislocation channels tend to be present on {1 1 1} and {1 0 0} glide planes.

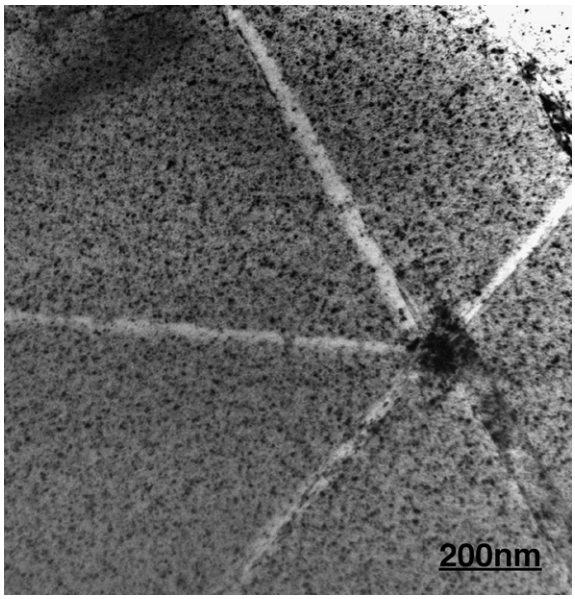

Fig. 3. Example of microstructure of dislocation channels in deformed 316SS irradiated to 0.78 dpa.

Table 1
Summary of observed defect clusters in neutron-irradiated 316SS

	Dose (dpa)	Frank loop		Black dot	
		Number density (m^{-3})	Mean size (nm)	Number density (m^{-3})	Mean size (nm)
316SS	0.01	–	–	8.0×10^{22}	1.5
	0.15	–	–	2.5×10^{23}	1.6
	0.79	1×10^{23}	3.5	3.0×10^{23}	1.8

On the assumption that all the grains in the material deformed uniformly and grain rotation during deformation is negligible, the resolved shear stress (RSS), τ_{rss}, for each dislocation channel observed was estimated by $\tau_{rss} = \sigma_{as}\cos(\phi)\cos(\theta)$, where σ_{as} is the applied stress, ϕ is the angle between the plane normal and the applied stress, and θ is the angle between the slip direction and the applied stress [2]. The dependence of the RSS on the angle between the tensile axis and either the slip plane normal or slip direction in each grain where channeling occurred was reported in a previous paper [7]. There is a tendency for the RSS to be the greatest when the angle is around 45° due to simple

geometrical considerations. The Schmid factor, m, is defined as the ratio of the resolved shear stress to the axial stress, $m = \cos(\phi)\cos(\theta)$. The maximum value of m occurs when the shear plane is at a 45° angle to the applied stress. Analysis of the dependence of measured dislocation channel width on the angle between the tensile axis and either the slip plane normal or the slip direction indicated that there is the same tendency as the RSS for the channel width to be wider when the angle is around 45°. Of potentially greater significance for understanding the deformation mechanisms in dislocation channeling, the channel width increased with increasing RSS as seen in Fig. 4. This indicates that the largest localized deformation tends to occur at the highest resolved shear stress level and that there may be a stress-dependent mechanism that limits the width of the dislocation channel evolution during deformation.

The association of deformation-induced martensite phase with dislocation channels was also observed in the deformed 316SS irradiated to higher than 0.1 dpa. As mentioned in Section 3.1, a prompt decrease and small increase of strain-hardening rate were observed in the deformed 316SS irradiated at higher irradiation doses, which is probably due to localized deformation. Microstructural analysis in the present study indicates that the prompt decrease of strain-hardening rate would be due to deformation with dislocation channeling. Several mechanisms could be responsible for the small increase of strain-hardening rate such as second phase formation and a long-range back stress. The martensite phase would be a barrier for moving dislocations in the channels, and therefore could be one reason for the small increase in strain-hardening rate.

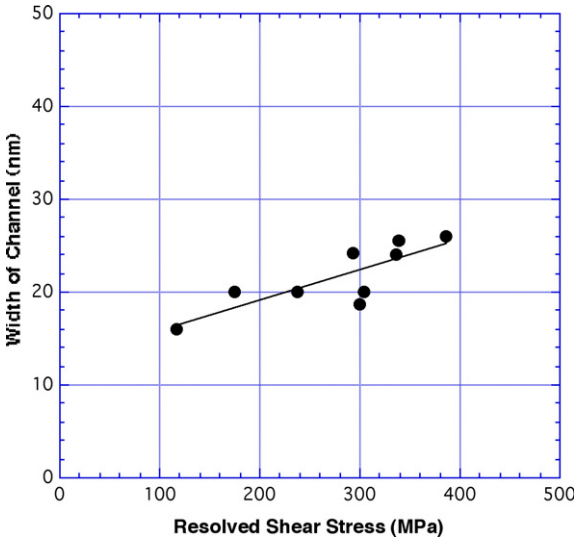

Fig. 4. Relationship between dislocation channel widths and the resolved shear stress.

Fig. 5 shows martensite phase formation at strain levels of 1.9%, 5.3%, and 32% in the deformed 316SS irradiated to 0.78 dpa. It should be noted that martensite formation was found at all strain levels at room temperature. The martensite phase was found at intersections of channels and/or twins on {1 1 1} planes with stacking faults as a result of localized deformation. The estimated RSS for each channel was less than 200 MPa, which is normally insufficient for martensite formation at room temperature [8]. It is suggested that a very high stress could be locally generated at intersections of channels leading to the localized martensite formation.

Diffraction pattern analysis revealed that a specific fcc (γ) and bcc (α martensite) orientation relationship resulted from the region of intersection of dislocation channels. No hcp phase (ε martensite) was found in this study. The bcc pattern has the zone axis $\langle 1\,0\,0\rangle_\alpha$ indicating N (Nishiyama) orientation relationship. The plastic deformation-induced transformation is to be thought of as a true mode of plastic deformation of the materials, concurrent with the plastic deformation modes of the parent phase [9]. It is convenient to use dislocation models to analyze these deformation processes. Actually, there are numerous mechanisms by which groups of dislocations suitable for martensitic nucleation by faulting can be produced by plastic deformation. The most obvious would be the stacking of dislocations at pile-ups involving several parallel slip planes. A mechanism for the formation of properly spaced dislocations by cross slip from planar pile-ups has found experimental support in the $\gamma \rightarrow \varepsilon$ transformation [10]. The $\gamma \rightarrow \varepsilon$ martensite formation is the simplest case for examining the concept of nucleation by a faulting mechanism, in that the entire transformation can be achieved by simple faulting. An ε crystal can be created from γ merely by the passage of a Shockley partial dislocation on every second close packed plane. In this study, however, no ε phase was found. The commonly observed strain induced nucleation of the $\gamma \rightarrow \alpha$ transformation [9,11] at various types of shear band intersections has already been rationalized in terms of the formation of the appropriate partial dislocations for the first Bogers–Burgers shear [9]. The first shear of the Bogers–Burgers model involves displacements on each $\langle 1\,1\,1\rangle_{\mathrm{fcc}}$ plane of $\frac{a_{\mathrm{fcc}}}{18}[1\,1\,2]$, i.e.,

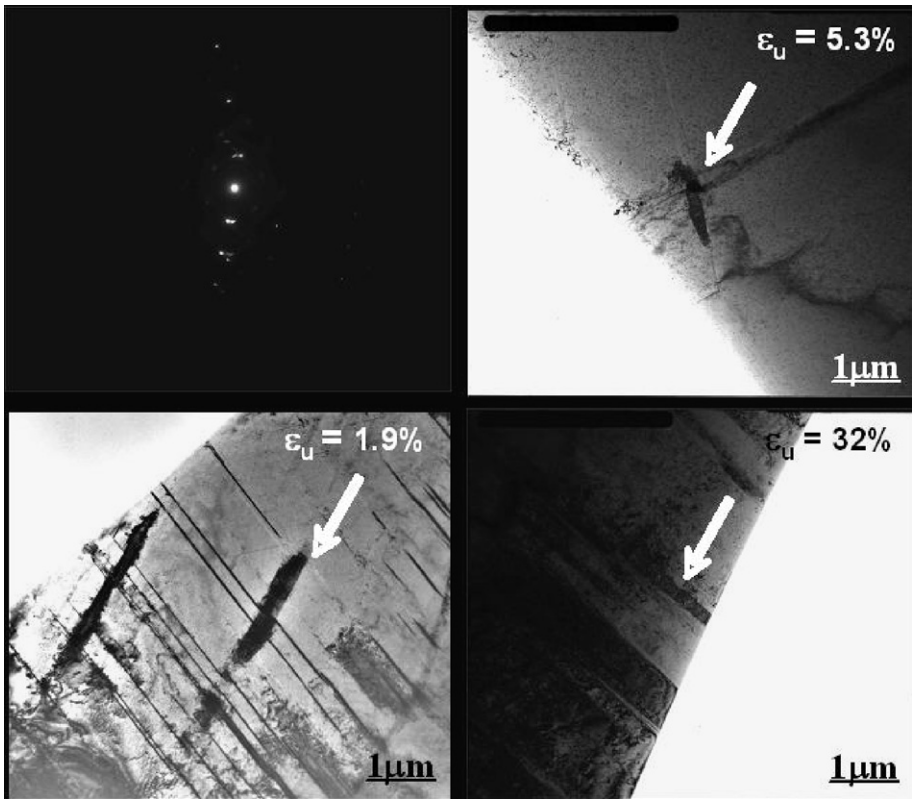

Fig. 5. Deformation-induced martensite formation located along with dislocation channels at various strain levels.

one-third the Burgers vector of a Shockley partial dislocation, $\frac{a_{fcc}}{6}[1\,1\,2]$. Bogers and Burgers have suggested that such partial displacements might occur by the spreading of a Shockley partial dislocation over a number of successive $\langle 1\,1\,1\rangle_{fcc}$ planes. However, the first shear only is considered to be the critical stage [12], the $\gamma \rightarrow \alpha$ transformation should be completed by a second shear and by the necessary accommodation. According to Lecroisey [9], nucleation of α martensite would take place at sites where the transformation mode of deformation is preferred to the parent phase mode. In this study, intersections of deformation bands, dislocation channels and/or twins on $\{1\,1\,1\}$ planes, have been shown to be favorable sites. These intersection sites are extremely favorable as transformation dislocations can be formed together with high stress concentrations resulting from piling-up of slip or twinning dislocations.

4. Conclusions

The deformation microstructure of an irradiated 316 stainless steel has been investigated by transmission electron microscopy in order to understand the deformation mechanisms of low stacking fault energy materials showing a loss of strain hardening capacity.

(1) Very high strain-hardening rates were found at the onset of deformation, and the strain-hardening rate decreased rapidly with increasing stress. In the 316SS unirradiated and irradiated to lower doses, the strain-hardening rate decreased with stress to the end of deformation.
(2) Irradiation-induced defect clusters, consisting predominantly of Frank loops in 316SS, were observed at the higher irradiation doses. The estimated barrier strength for defect clusters in the materials was in good agreement with previously reported values.
(3) Dislocation channeling occurred in the specimens irradiated to 0.1–0.78 dpa, and is coincident with prompt plastic instability at yield. Channel width seems to be wider when the angle between tensile direction and dislocation slip direction is close to 45°, corresponding to the maximum resolved shear stress condition.

(4) Deformation-induced martensite phase was found at all investigated strain levels at room temperature and tends to be found mainly at intersections of channels. It is suggested that a very high stress would be locally generated at intersections of channels leading to the localized $\gamma \rightarrow \alpha$ martensite formation by the spreading of a Shockley partial dislocation over a number of successive $\langle 1\,1\,1 \rangle_{fcc}$ planes.

Acknowledgement

This research was sponsored by the Office of Fusion Energy Sciences, US Department of Energy, under contract No DE-AC05-00OR22725 with UT-Battelle, LLC.

References

[1] S.J. Zinkle, Radiat. Eff. Def. Solids 148 (1999) 447.
[2] N. Hashimoto, T.S. Byun, K. Farrell, S.J. Zinkle, J. Nucl. Mater. 336 (2005) 225.
[3] N. Hashimoto, T.S. Byun, K. Farrell, S.J. Zinkle, J. Nucl. Mater. 329–333 (2004) 947.
[4] T.S. Byun, K. Farrell, N. Hashimoto, J. Nucl. Mater. 329–333 (2004) 998.
[5] N. Hashimoto, S.J. Zinkle, A.F. Rowcliffe, J.P. Robertson, S. Jitsukawa, J. Nucl. Mater. 283–287 (2000) 528.
[6] N. Hashimoto, E. Wakai, J.P. Robertson, J. Nucl. Mater. 273 (1999) 95.
[7] N. Hashimoto, T.S. Byun, K. Farrell, J. Nucl. Mater., in press.
[8] G.B. Olson, M. Cohen, Metall. Trans. 7A (1976) 1905.
[9] F. Lecroisey, A. Pineau, Metall. Trans. 3 (1972) 387.
[10] J.B. Cohen, J. Weertman, Acta Met. 11 (1963) 996.
[11] P.L. Manganon, G. Thomas, Metall. Trans. 1 (1970) 1577.
[12] W.G. Burgers, J.A. Klostermann, Acta Met. 13 (1965) 568.